URSI AP-RASC 2019, New Delhi, India, 09 - 15 March 2019

On the Quantification of the Uncertainty of an Electromagnetic Prediction – An Application with Experimental Verification

Carlo F.M. Carobbi
Department of Information Engineering, University of Florence, 50139, Firenze, Italy, carlo.carobbi@unifi.it

Abstract

It is here described the procedure followed to predict the electromagnetic field radiated by an active broadband antenna in different electromagnetic environments (fully- and semi-anechoic) and assuming different measurement methods (with or without height scanning of the receiving antenna). Prediction includes a best estimate and uncertainty. An experimental confirmation of the validity of the prediction is provided.

1. Introduction

Quantification of measurement uncertainty is a consolidated practice whenever the measurement result is used for conformity assessment or it has scientific significance. The Guide to the Expression of Uncertainty in Measurement (GUM, [1]) and its supplements provide authoritative and well established methods for quantification of measurement uncertainty. The scope of this contribution is to show an application where the uncertainty of an electromagnetic prediction is quantified through the same methods used to quantify uncertainty in measurements and based on a model equation (a prediction model rather than a measurement model) and propagation of uncertainty from the model input to the model output quantities. Confirmation of the validity of the prediction result, which similarly to a measurement result consists of a best estimate and expanded uncertainty, is provided through comparison with a measurement result. The comparison is performed by evaluating the compatibility between prediction and measurement results. It is acknowledged that a standard method, named "feature selective validation" [2] is available for validating an electromagnetic simulation which is extensively used by the research community in the field of electromagnetic compatibility (see [3] and [4] for a recent review of the method). It is here stressed however the importance of using, whenever possible, methods for validating a prediction result that are consistent with those used in metrology and characterized by a direct and solid interpretation.
In section 2 the electromagnetic problem under investigation is introduced and the procedure for predicting the quantity of interest is described. The comparison between prediction and measurement results is the subject of section 3.

2. Prediction of the electromagnetic field generated by an active broadband antenna

A reference electromagnetic field source was manufactured for the purpose of realizing a travelling sample for interlaboratory comparison of radiated emission measurements. The sample consists of the combination of a comb generator and a biconical antenna, see Figure 1.

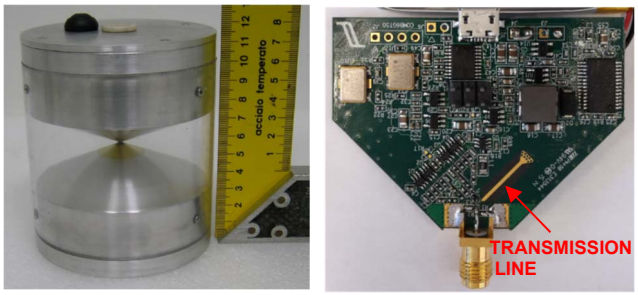

(a) (b)

Figure 1. Biconical antenna (a) and comb generator (b). The comb generator feeds the biconical antenna and it is assembled inside the top cone.

The structure and operation of the sample is described in [5], while its application in interlaboratory comparisons is reported in [6]. The scope here is to provide information on the original calibration procedure and on quantification of the uncertainty of the predicted radiated field.
For sake of brevity the comb generator calibration is not described here. The result of this calibration, in terms of the power that each harmonic of the comb generator delivers to a 50 Ω load, is characterized by a probability density function (PDF) that was numerically obtained through application of the GUM Supplement 1 (GUMS1) numerical method [7], based on Monte Carlo random sampling. The comb generator power that each of the 120 harmonics (at 50 MHz steps, from 50 MHz to 6 GHz) delivers to a 50 Ω load is represented by the same numerical PDF shifted at the best estimate of the power associated with the specific harmonic frequency. The standard uncertainty of the PDF is bell-shaped, its standard uncertainty is 0.33 dB and the expanded uncertainty (corresponding to 95 % coverage probability) is 0.62 dB.

A commercial electromagnetic simulation tool was used, together with the result of the calibration of the comb generator, to predict the electric field radiated by the sample. The numerical algorithm adopted by the tool is based on the finite integral technique, which consists in the time domain solution of Maxwell integral equations over a finite size, discretized volume surrounding the radiator at

discrete time steps. A comparison was carried out with a second simulation tool based on the method of moments (MoM) in frequency domain in order to verify the obtained degree of accuracy of the numerical predictions.

Three electromagnetic configurations were analyzed for the radiated field, all of them in vertical polarization: 3 m distance in free-space (fully anechoic environment, from 50 MHz to 6 GHz), 3 m and 10 m distance, with the base of the sample at 80 cm above a perfectly reflecting and infinite ground plane (semi-anechoic environment, from 50 MHz to 1 GHz). The maximum of the electric field in the height range between 1 m and 4 m was calculated in the semi-anechoic environment, as required by the applicable EMC standard [8].

A. Fully anechoic environment

A cubic volume of 1.5 m side and centered on the sample was discretized in about $43 \cdot 10^6$ hexahedral cells having a side comprised between 0.1 mm and 2 mm. Allowance for cell refinement around the corners of the sample was provided. Appropriate boundary conditions were set at the borders of the volume to simulate free space. Electric and magnetic symmetry was employed to reduce memory occupation and computation time. The time step corresponding to the adopted resolution of the space discretization was 1.18 ps and the analyzed time interval was about 11 ns, i.e. well beyond the duration of the impulse response of the biconical antenna. The total computation time on a portable PC was about ninety minutes.

All the relevant geometrical and physical (material) details of the biconical antenna were implemented in the computer design. The accurate description of the feeding of the biconical antenna was particularly critical due to its impact on the prediction of mismatch.

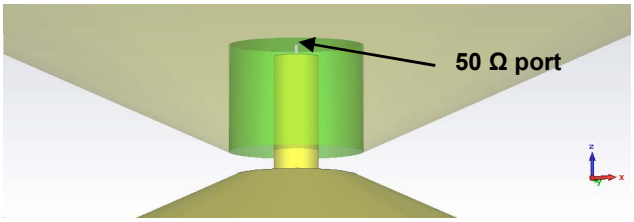

Figure 2. Detail of the transition from the comb generator output reference plane to the biconical antenna input, as implemented in the computer design.

The actual transition from the reference plane of the comb generator output to the input of the biconical antenna, consisting in a coaxial structure with rexolite as insulating material, was implemented in the computer design, see Figure 2. The feeding is realized through a 50 Ω port connected between the inner coaxial conductor and the inner surface of the top cone (see Figure 2). As a reference for dimensions in Figure 2 note that the size of the gap between the tips of the cones is 0.55 mm. The simulation model equation is given by

$$E = E_{sim} + P_c - 30 - M_a + \delta E + \delta P. \qquad (1)$$

where E is the predicted electric field (in dB(μV/m)), E_{sim} is the electric field that results from the simulation (in dB(μV/m)), P_c is the comb generator output power (in dBm), 30 (in dBm units) corresponds to the value of power set in simulations for feeding the biconical antenna (1 W), $M_a = 20\log|1 - \Gamma_c\Gamma_a|$ is the mismatch error correction (Γ_c is the measured output reflection coefficient of the comb generator and Γ_a is the reflection coefficient of the biconical antenna as seen from the 50 Ω port in Figure 2), δE is a correction that takes into account the unavoidable deviation between the actual geometry of the biconical antenna and the one implemented in the computer design, δP is a correction associated to the deviation between the power generated by the comb generator during the calibration and when mounted inside the cone.

E_{sim} is affected by an error due to the numerical method on which the simulation tool is based and the chosen settings. This error was evaluated performing the simulation of the same computer design with another simulation tool based on MoM in frequency domain (i.e. an independent numerical method). The maximum deviation between the two simulations was less than 0.5 dB over the full frequency range from 50 MHz to 6 GHz. The maximum deviation associated with the correction δE was evaluated by performing a set of parametric simulations assuming different dimensions of the biconical antenna. It was realized that the parameter on which the simulated electric field is mostly sensitive is the gap between the tips of the cones, the one which is also less easily controllable when assembling the antenna. The interval of the possible values of the gap size was estimated to be within 0.4 mm and 0.7 mm and four simulations were carried out at 6 GHz assuming a gap size of 0.4, 0.5, 0.6 and 0.7 mm. The corresponding range of the values of the simulated electric field was less than 0.6 dB. Finally, the maximum deviation associated with the correction δP was estimated measuring the comb generator power in absence and in presence of a nearby grounded metallic structure. The metal enveloped the comb generator close to its terminals for the purpose of reproducing the effect of the coupling with the inner surface of the cone hosting the generator. The comb generator power was mostly sensitive to the presence of the surrounding metal in the frequency range between 5.2 GHz and 5.8 GHz. It is interesting to note that the shorted transmission line that is alternatively charged and discharged to generate the repeated impulses at the output of the comb generator, see Figure 1(b), is one fourth of wavelength at about 5.5 GHz.

The uncertainty of the predicted electric field was quantified by using the Monte Carlo numerical technique along the guidelines offered by the GUMS1 and based on the simulation model (1). The corresponding uncertainty budget is shown in Table I. Note that the PDF of P_c is the one numerically obtained through comb generator power calibration.

$\overline{E_{sim}}$ is the average value of the simulated electric field resulting from the parametric (at varying gap size) analysis. The dominant contribution to the uncertainty of the prediction is mismatch. The maximum of the product

$|\Gamma_c \Gamma_a|$ over the full 50 MHz to 6 GHz frequency was evaluated to be 0.14. The corresponding limits of a U-shaped PDF are ±1.23 dB. Finally, the standard uncertainty of the predicted electric field turns out to be 1.00 dB and the expanded uncertainty, corresponding to 95 % coverage probability, is 1.78 dB (worst case from 50 MHz to 6 GHz).

Table I. Electric Field Prediction Uncertainty Budget.

Quantity	Measurement unit	PDF	Mean	Standard uncertainty (dB)
$\boldsymbol{E_{sim}}$	dB(μV/m)	$R(\overline{E_{sim}} \pm 0.5)$	$\overline{E_{sim}}$	0.29
$\boldsymbol{P_c}$	dB	$PDF\ (P_c)$	$\bar{P}_c$	0.33
30	dBm	---	30	0
$\boldsymbol{M_a}$	dB	$U(\pm 1.23)$	0	0
$\boldsymbol{\delta E}$	dB	$R(\pm 0.3)$	0	0.17
$\boldsymbol{\delta P}$	dB	$R(\pm 0.3)$	0	0.17
$\boldsymbol{E}$	dB(μV/m)	$PDF\ (E)$	$\bar{E}$	1.00

B. Semi-anechoic environment

We skip the details of the simulation settings for the semi-anechoic environment, which are similar to those used for the fully anechoic environment. It is instead worth mentioning the line of reasoning followed to get insight into the simulation results and assign an uncertainty figure to them. It is reasonable to assume, due to the physics of the electromagnetic problem, that the biconical antenna radiates in the semi-anechoic environment as in the fully anechoic one. More specifically the input impedance and radiation pattern of the antenna are not expected to significantly change when passing from an environment to the other. Further, the receiving antenna is in the far field of both the biconical antenna and its image. Then it is expected that the electric field generated by the biconical antenna in the semi-anechoic environment is obtained through scaling the electric field predicted in the fully anechoic environment by a factor that depends only on geometry and frequency and given by

$$K_v = d_3 \left| \frac{e^{-j\beta r}}{r}\left(\frac{d}{r}\right)^2 + \frac{e^{-j\beta r'}}{r'}\left(\frac{d}{r'}\right)^2 \right|_{max}, \qquad (2)$$

where $d_3 = 3$ m, d is 3 m or 10 m, r is the distance between the biconical antenna and the point where the field is measured, r' is the same distance but from the image of the biconical antenna, $\beta = 2\pi/\lambda$ and λ is the wavelength. (2) applies to the adopted vertical polarization and to a dipole like ($\sin\theta$) radiation pattern, which is indeed, to a good approximation, the shape of the pattern of the biconical antenna up to 1 GHz. The maximum is taken over the scanning height of the receiving antenna, i.e. 1 m to 4 m as required in [8]. It turns out that the ratio of the simulated fields in the semi-anechoic and fully anechoic environments deviates from (2) by no more than 0.40 dB (from 50 MHz to 1 GHz, for both the 3 m and 10 m distances). Hence, attaching this worst case 0.40 dB deviation to the uncertainty of the prediction in the semi-anechoic environment, only a slightly larger uncertainty results. This larger uncertainty is estimated as $\sqrt{\left(\frac{0.4}{\sqrt{3}}\right)^2 + 1^2} = 1.03$ dB in terms of one standard deviation, or 1.85 dB in terms of expanded uncertainty (corresponding to a coverage probability of 95 %).

3. Confirmation of prediction results

The electric field prediction results were validated through a comparison with measurement results. Measurements were carried out in a fully anechoic chamber at 3 m distance from the sample in the frequency range from 350 MHz to 6 GHz, where the imperfection of the chamber is tolerable. The prediction at the six frequencies from 50 MHz to 300 MHz was validated through comparison with near-field magnetic field measurements which were performed by using a highly symmetric loop antenna. These near field measurements provided an indirect confirmation of the validity of the prediction, assuming that the predictions have the same degree of accuracy both in the far-field and in the near-field. This is reasonable because the far-field predictions at locations outside the discretized volume are obtained from near-field (i.e. inside the volume) predictions.

We here briefly present the results of the measurements in the far field (i.e. in the fully anechoic chamber) and the comparison with predictions. Measurements were carried out by using three different types of antennas in order to cover the frequency range from 350 MHz to 6 GHz, namely a log-periodic dipole array from 350 MHz to 3 GHz (band #1) and two standard-gain horns, one from 3050 MHz to 4000 MHz (band #2) and another one from 4050 MHz to 6000 MHz (band #3). The reason behind the selection of these antennas is their relatively high gain, compared with other available (e.g., compact biconical) antennas. The advantages associated with the high gain are a relatively small sensitivity to anechoic chamber imperfections and a relatively high received power over the noise floor of the receiver (a good quality spectrum analyzer).

The measurement model equation is

$$E_m = V_{sa} + A + AF + M_m + \delta SA, \qquad (3)$$

where E_m is the measured electric field, V_{sa} is the voltage indicated by the spectrum analyzer, A is the attenuation of the cable connecting the receiving antenna to the spectrum analyzer, AF is the antenna factor of the receiving antenna, M_m is the mismatch error correction and δSA is the correction for spectrum analyzer inaccuracy. The measurement uncertainty budget is shown in Table II. Where three values are shown then the first applies to band #1, the second to band #2 and the third to band #3. When a single value is shown then it applies to the full frequency range.

Table II. Fully Anechoic Chamber Electric Field Measurement Uncertainty Budget.

Quantity	Measurement unit	PDF	Mean	Standard uncertainty (dB)
V_{SA}	dB(μV)	$t_2\left(\overline{V_{SA}}, \frac{0.57}{\sqrt{3}}\right)$ $t_2\left(\overline{V_{SA}}, \frac{0.27}{\sqrt{3}}\right)$ $t_2\left(\overline{V_{SA}}, \frac{0.44}{\sqrt{3}}\right)$	$\overline{V_{SA}}$	0.33 0.16 0.25
A	dB	$N(\bar{A}, 0.06)$	$\bar{A}$	0.06
AF	dB(1/m)	$N(\overline{AF}, 0.35)$ $R(\overline{AF} \pm 0.3)$ $R(\overline{AF} \pm 0.3)$	$\overline{AF}$	0.35 0.17 0.17
M_m	dB	$R(\pm 1.0)$ $R(\pm 0.5)$ $R(\pm 0.5)$	0	0.58 0.29 0.29
δSA	dB	$N(0,0.23)$ $N(0,0.71)$ $N(0,0.71)$	0	0.23 0.71 0.71
E_m	dB(μV/m)	$PDF\ (E_m)$	$\bar{E}$	0.98 0.92 1.01

The measurement uncertainty due to the imperfection of the anechoic chamber was attached to the quantity V_{SA}. In order to evaluate this uncertainty contribution the receiving antenna was moved horizontally along the line passing through the center of phase of the receiving and the transmitting (sample) antenna and vertically. The voltage received was then corrected for the far-field 1/distance decay and the deviation from the voltage received at the reference (3 m distance) position was evaluated. The displacements were 10 cm (along vertical) and 20 cm (along horizontal). A shifted and scaled Student's *t* PDF was assigned to this uncertainty contribution, as indicated in the second row of Table II.

The expanded uncertainty of the measured electric field obtained through application of the GUMS1 procedure and corresponding to a coverage probability of 95 % was 1.92 dB in band #1, 1.80 dB in band #2 and 1.98 dB in band #3. The result of the comparison between measured and predicted values of the electric field is shown in Figure 3. Results are reported in term of deviation from the predicted values. Different colors correspond to different bands (as detailed in the legend). The length of the error bars is two-times the expanded measurement uncertainty. The range of the interval delimited by the black horizontal lines is two times the expanded prediction uncertainty. Full compatibility results thus providing confidence on the validity of both measurements and predictions.

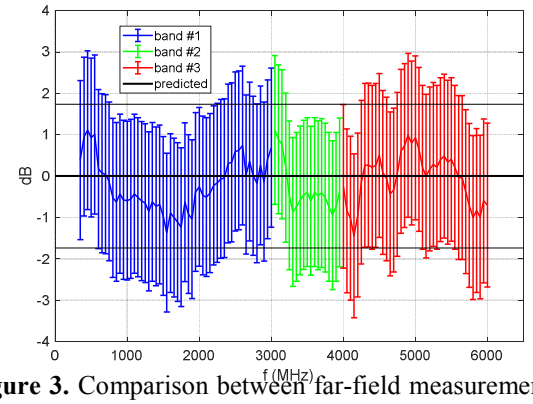

Figure 3. Comparison between far-field measurements in a fully-anechoic chamber and the corresponding predictions.

4. References

1. BIPM, IEC, IFCC, ILAC, ISO, IUPAC, IUPAP and OIML, 2008 Guide to the Expression of Uncertainty in Measurement, JCGM 100:2008, GUM 1995 with minor corrections.

2. IEEE Std 1597.1-2008, "IEEE Standard for Validation of Computational Electromagnetics Computer Modeling and Simulations."

3. Alistair P. Duffy, Antonio Orlandi and Gang Zhang, "Review of the Feature Selective Validation Method (FSV). Part I—Theory," *IEEE Transactions on Electromagnetic Compatibility*, vol. 60, issue 4, 2018, pp. 814-821.

4. Alistair P. Duffy, Antonio Orlandi and Gang Zhang, "Review of the Feature Selective Validation Method (FSV). Part II—Performance Analysis and Research Fronts," *IEEE Transactions on Electromagnetic Compatibility*, vol. 60 , issue 4, 2018, pp. 1029-1035.

5. Alessio Bonci, Enrico Boni, and Carlo F. M. Carobbi, "A Compact, Broadband, Calculable Electromagnetic Field Source for Quality Assurance in EMC Testing," IEEE Transactions on Electromagnetic Compatibility, vol. 60, no. 5, pp. 1215 – 1222, Oct. 2018.

6. Carlo F. M. Carobbi, Alessio Bonci, Marco Cati, Carlo Panconi, Michele Borsero and Giuseppe Vizio, "Proficiency Testing by Using Traveling Samples With Preassigned Reference Values", IEEE Transactions on Electromagnetic Compatibility, vol. 58, no. 4, pp. 1339 – 1348, Aug. 2016.

7. BIPM, IEC, IFCC, ILAC, ISO, IUPAC, IUPAP and OIML, 2008 Supplement 1 to the 'Guide to the Expression of Uncertainty in Measurement' – Propagation of distributions using a Monte Carlo method, JCGM 101:2008.

8. Specification for radio disturbance and immunity measuring apparatus and methods - Part 2-3: Methods of measurement of disturbances and immunity - Radiated disturbance measurements, CISPR 16-2-3:2016.